



# Wheelset-Track Dynamic Interaction Modelling with Frequency- and Preload-Dependent Stiffness and Damping of Resilient Track Components

Andrea Collina, Roberto Corradi , Egidio Di Gialleonardo , and Qianqian Li  

Politecnico di Milano, Milan 20156, MI, Italy  
qianqian.li@polimi.it

**Abstract.** Resilient track components are widely used in the modern railway tracks, such as the rail pads, the sleeper pads, the continuous support of the embedded rail system (ERS), etc. Track components made of resilient materials usually possess non-linear dynamic properties. In the present work, the equivalent stiffness and damping of an ERS are characterised in function of preload and frequency through laboratory tests and show an obvious non-linear behaviour. A non-linear rheological model of unit length of the ERS is identified according to the experimental data. The good agreement between the identified and experimental equivalent stiffness and damping proves the rheological model an appropriate way for the modelling of the non-linear properties of the ERS. The rheological model is subsequently integrated into a 2D track model of wheelset-track dynamic interaction simulation. The simulation related to a wheelset passage is performed and the results are compared to the ones obtained with a linear track model. The system responses obtained with the linear and non-linear track models are considerably different from each other. The results imply that the non-linear dynamic properties of resilient track components should be carefully analysed and accounted for in the train-track dynamic interaction when an accurate prediction of the system response is desired.

**Keywords:** Track nonlinearities · Non-linear track rheological model · Train-track dynamic interaction

## 1 Introduction

When using numerical models to study the train-track dynamic interaction and the relevant issues, it is important to properly model the dynamic characteristics of the involved subsystems and components. Most of the train-track dynamic interaction models proposed in the literature (e.g. [1–4]) rely on linear track models. However, when track components with a strong non-linear dynamic property are employed, such as resilient materials, the track model should be able to account for the non-linear dynamic characteristics in the train-track dynamic interaction for a precise prediction of the track

and vehicle response. In fact, resilient track components such as rail pads, sleeper pads or the continuous elastic support in embedded rail systems, show significant variations of their dynamic stiffness with dynamic load amplitude, frequency and preload [5–7]. Research have been carried out to seek for proper models to consider the non-linear dynamic properties of track components, also for other similar components in general, in time domain. Berg [8] used a three-parameter Zener model in parallel with a friction force model for rubber springs. The model is able to describe the dependence of the dynamic properties on frequency and also the non-linear behaviour related to friction force. As another alternative, Fenander [9] used a combination of a fractional derivative element and a cubic function to model the dynamic properties of a rail pad. The fractional derivative element results in a frequency-dependent stiffness and damping while the cubic function describes the dependence of stiffness on static preload. A similar approach is employed later by Zhu et al. [10].

A non-linear rheological model able to reproduce the frequency- and preload-dependent stiffness and damping of resilient track components was proposed and validated in a previous study [11]. In this paper, the dynamic characteristics of an embedded rail system (ERS) are investigated through laboratory tests. The experimental data is then used to identify a non-linear rheological model of unit length of the tested ERS. The identified rheological model is subsequently integrated into a 2D track model in the vertical plane. Wheelset-track dynamic interaction simulation is performed with the developed non-linear track model. To better understand the effect of the non-linear track model on the system response, simulation results are compared to the ones obtained with a linear track model.

## 2 Experimental Tests

The laboratory tests to investigate the dynamic characteristics of the ERS were carried out on a 750 mm long full-scale sample in the labs of Politecnico di Milano. The experimental test setup is illustrated in Fig. 1.

The ERS bounds the rail with resilient materials and enclose them with a steel channel (the red part clamped on the ground). A hydraulic actuator applies an input force on the rail head in the middle of the sample. The resultant rail displacement is measured by 4 laser sensors distributed on the two sides of the sample. The quasi-static tests were carried out in accordance with the requirements of the reference technical standards [12]. The dynamic tests with an harmonic force input were performed with different frequencies (1, 3, 5, 10, and 20 Hz) and preloads (6, 18, 37, and 55 kN where 55 kN corresponds to the maximum static deflection induced by a single bogie of a SCHIMMNS freight wagon) with a 5 kN amplitude.

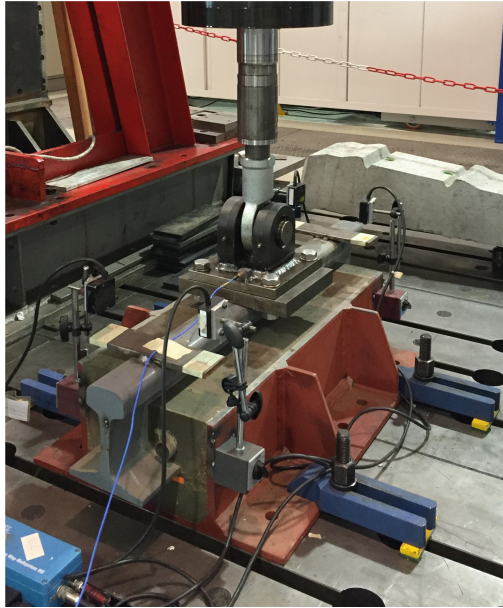


**Fig. 1.** Test bench for the experiments on a full-scale 750 mm long ERS sample.

The static stiffness of unit length of the tested ERS is characterised as  $60 \text{ MN m}^{-2}$ . The equivalent stiffness and damping of unit length obtained from the dynamic tests are reported in Fig. 2.

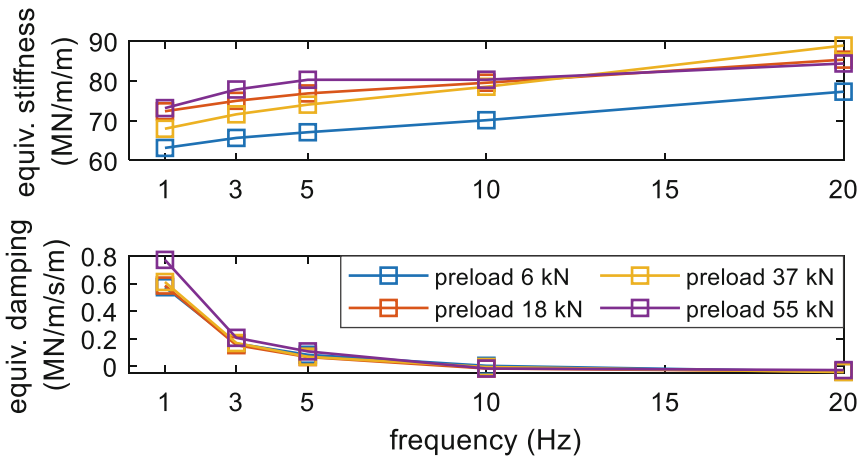


**Fig. 2.** Laboratory experiment results of the equivalent stiffness (upper plot) and damping (lower plot) of unit length of the tested ERS in function of preload and frequency.

It can be observed that the preload and frequency of the input force lead to considerable changes in the equivalent stiffness and damping of the ERS. In particular, the equivalent stiffness increases with the frequency while the equivalent damping decreases rapidly with the frequency.

### 3 Numerical Models

#### 3.1 ERS Non-linear Rheological Model

The non-linear rheological model of unit length of the tested ERS is a Zener model with 3 parameters (the scheme is presented in Fig. 3): a spring ( $k_1$ ) in parallel with a combination of a spring ( $k_2$ ) and a damper ( $c_2$ ) in series [13].

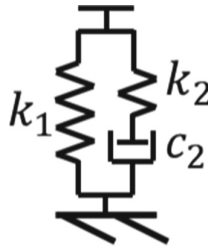


**Fig. 3.** The non-linear rheological model of unit length of the tested ERS: a Zener model with 3 parameters.

All three parameters ( $k_1, k_2, c_2$ ) are in function of preload ( $P$ ) and are defined as:

$$\begin{aligned}
 k_1 &= k_{1,0}(1 + P/P_0)^x \\
 k_2 &= k_{2,0}(1 + P/P_0)^x \\
 c_2 &= c_{2,0}(1 + P/P_0)^x
 \end{aligned}
 \tag{1}$$

where  $k_{1,0}, k_{2,0}, c_{2,0}$ , are constant reference values of  $k_1, k_2$  and  $c_2$ ;  $P$  is the preload applied on the ERS;  $P_0$  is a constant reference preload and  $x$  is a non-dimensional constant number.

$k_{1,0}, k_{2,0}, c_{2,0}$  and  $x$  are determined through a minimisation procedure of the difference between the modelled and experimental equivalent stiffness and damping for all test frequencies and preloads. The constant reference preload  $P_0$  is set as 64 kN. The objective function of the minimisation procedure is defined as

$$err = \sum_{i=1}^{n_p} \sum_{j=1}^{n_\Omega} \left[ (k_{equiv.,num.}(P_i, \Omega_j) - k_{equiv.,exp.}(P_i, \Omega_j))^2 + 10(c_{equiv.,num.}(P_i, \Omega_j) - c_{equiv.,exp.}(P_i, \Omega_j))^2 \right]
 \tag{2}$$

where  $i$  and  $j$  are the indices of the preload case and test frequency respectively;  $n_p$  and  $n_\Omega$  are the total number of the preload cases and test frequencies respectively;  $k_{equiv.,num.}$  and  $c_{equiv.,num.}$  are the equivalent stiffness and damping computed by the numerical model while  $k_{equiv.,exp.}$  and  $c_{equiv.,exp.}$  are the equivalent stiffness and damping computed

by the experimental results. A weight of 10 is applied to the modelling error of the equivalent damping with respect to the equivalent stiffness for a better performance of the minimisation procedure due to the difference between the orders of magnitude of the two parameters. The identified model parameter values are:  $k_{1,0} = 62 \text{ MN/m/m}$ ,  $k_{2,0} = 9.6 \text{ MN/m/m}$ ,  $c_{2,0} = 0.7 \text{ MN/m/s/m}$ ,  $x = 0.21$ . The comparisons of the experimental and modelled equivalent stiffness and damping are reported in Fig. 4.

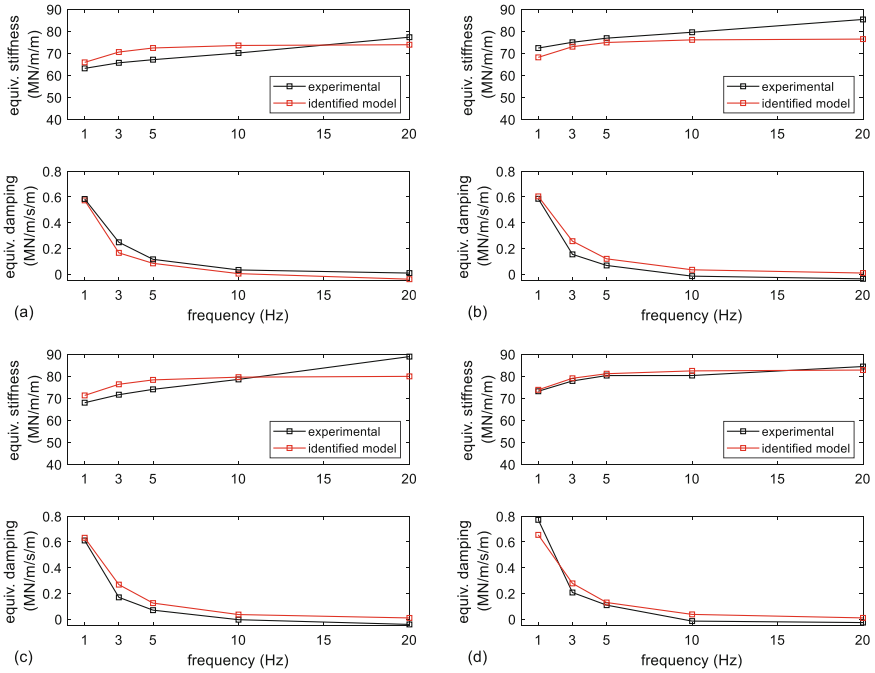


**Fig. 4.** Modelled and experimental equivalent stiffness (upper plot of each part) and damping (lower plot of each part) of unit length of the tested ERS: (a) preload = 6 kN; (b) preload = 18 kN; (c) preload = 37 kN; (d) preload = 55 kN.

Figure 4 shows that the modelled equivalent stiffness and damping are quite similar to the experimental ones, in terms of both the absolute values and the variation trend as a function of preload and frequency. Therefore, it is demonstrated that the non-linear rheological model is an appropriate way for the modelling of the equivalent stiffness and damping of the tested ERS. The equivalent stiffness at the same frequency increases with the preload. In fact, also the equivalent damping increase but the degree is relatively low.

Furthermore, the non-linear rheological model is able to predict the response of the tested ERS sample with a general input through a time domain simulation. In Ref. [8], the force applied by the hydraulic actuator to realise a desired rail displacement is measured and compared to a corresponding prediction simulated by the non-linear rheological model. The experimental measurement and the numerical prediction are

regarded highly similar. The difference between the maximum force values, which is the most significant point for the comparison, is about 4%.

To understand the possible effect of the modelled non-linear dynamic properties of resilient materials could have on the train-track dynamic interaction, a model of unit length of the tested ERS is developed. A rigid mass, representing unit-length of the embedded UIC 60 type rail, is added on the top of the non-linear rheological model of the reference ERS (Fig. 3). A harmonic load of 1 kN, superposed with a static preload, is applied to the rigid mass and the rail response, obtained by time domain integration, is compared to the one obtained with a linear model, where the model of the resilient material is substituted with a linear Kelvin-Voigt model. The constant stiffness and damping of the linear model are set as 80 MN/m/m and 0.001 MN/m/s/m.

The amplitude ratio of steady-state rail response to the harmonic force, as well as the phase delay, are computed and presented in Fig. 5. In the left part, the results obtained with a preload of 6 kN is compared to the ones of the linear in the frequency range of 0–500 Hz while in the right part, the results obtained with a preload of 6, 18, 37, and 55 kN are presented in the frequency range of 150–210 Hz.

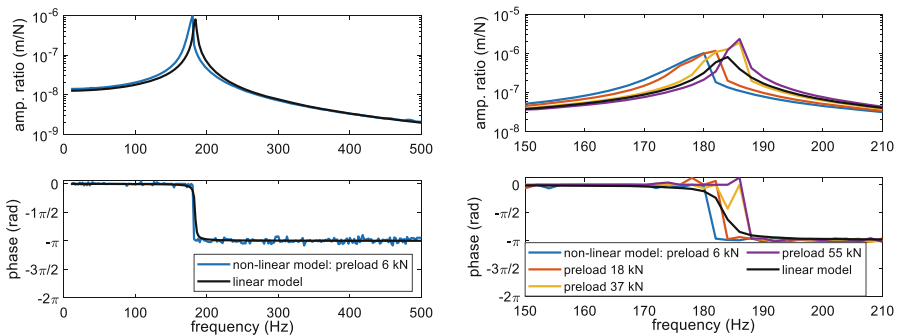


**Fig. 5.** Amplitude ratio (upper plot of each part) of the steady-state rail responses to the harmonic force and the phase delay (lower plot of each part), obtained with time domain simulation by linear and non-linear mechanical models of unit length of the ERS: (left) preload of 6 kN and dynamic force amplitude of 1 kN; (right) preload of 6, 18, 37, and 55 kN, and dynamic force amplitude of 1 kN.

The equivalent stiffness of the non-linear model increases with the preload and therefore also the frequency which corresponds to the peak of the amplitude ratio. On the other hand, the non-linear model provides a much lower damping at high frequency comparing to the linear model. Consequently, the peak values of the amplitude ratio of the non-linear model are always higher than the linear model.

### 3.2 Non-linear Track Model and Wheelset-Track Interaction Simulation

The non-linear wheelset-track dynamic interaction model is presented in Fig. 6.

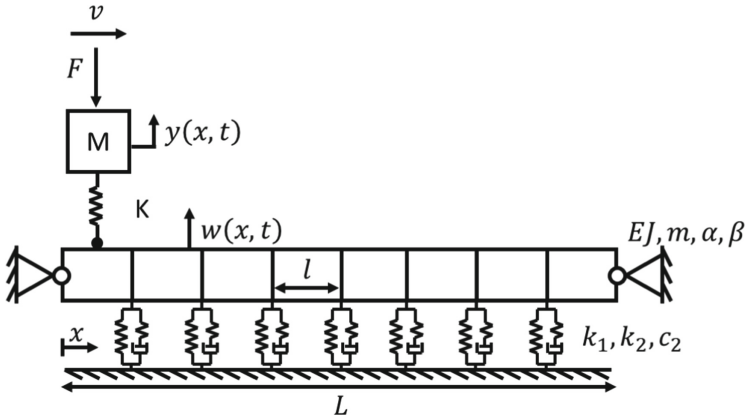


**Fig. 6.** Wheelset-track dynamic interaction model which consists in a 2D FE track model with non-linear foundation, a moving wheelset and a linear contact spring.

The model consists in a 2D FE track model with non-linear foundation, a moving wheelset and a linear Hertzian contact spring. The rails are modelled as FE Euler-Bernoulli beams. The non-linear foundation is modelled by a set of non-linear rheological models of the resilient material under the FE nodes and connected to the ground. The wheelset departs from the left boundary of the model and moves rightwards with a constant speed. The simulation input associated with the wheel/rail irregularity is not accounted for and will be considered in an updated version of the train-track interaction model. The track model has a finite length ( $L$ ) of 160 m. The data of the rail (bending stiffness  $EJ$ , mass per unit length  $m$ ) refer to the UIC 60 type. The Rayleigh damping parameters of the rail ( $\alpha$ ,  $\beta$ ) are set to 0 and  $2e-5$  respectively. The calculations of  $k_1$ ,  $k_2$  and  $c_2$  are presented in Eq. (1). It should be noted that the  $k_{1,0}$ ,  $k_{2,0}$  and  $c_{2,0}$  identified by the experimental results refer to the unit-length of the tested ERS. Therefore, when calculating  $k_1$ ,  $k_2$  and  $c_2$  for each non-linear rheological model connected to mesh nodes, the rail mesh size should be multiplied to the identified  $k_{1,0}$ ,  $k_{2,0}$  and  $c_{2,0}$ . Since the force applied on each non-linear rheological model is not a combination of a static preload and a mono-harmonic force, the static preload  $P$  in the calculation of  $k_1$ ,  $k_2$  and  $c_2$  are substituted by the instantaneous load applied on each non-linear rheological model. The wheelset mass ( $M$ , approximately 1500 kg) and the wheelset load ( $F$ , approximately 110 kN) refer to a passenger coach of train ETR 500. The wheelset speed is set to 200 km/h and the stiffness of the linear Hertzian contact spring is set to  $1e9$  N/m for a single wheel. The responses of the rails and the wheelset are obtained by time-domain numerical integration. The Newmark method is employed for the numerical integration with an integration step of  $2e-5$  s. No initial conditions are assigned to the rails.

To understand the effect of employing the non-linear foundation in the track model, simulation results are compared to the ones obtained by a linear track model. In the latter case, a continuous linear Kelvin-Voigt foundation replaces the non-linear foundation of Fig. 6. The values of the stiffness and damping per unit length are set to  $80$  MN  $m^{-2}$  and  $0.001$  MN  $m^{-2}$  s respectively. The time histories of the rail deflection at mid-span are compared in Fig. 7.

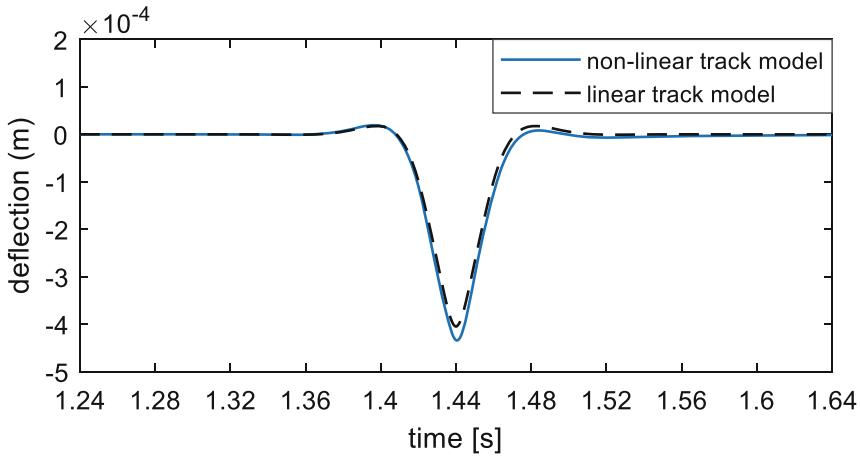


**Fig. 7.** Rail deflections at mid-span of the track models corresponding to a passage of the wheelset of an ETR 500 train at 200 km/h, obtained with linear and non-linear track models.

The results shown in Fig. 7 are limited to a time window of 0.4 s centred at the time instant when the wheelset passes mid-span (1.44 s) because the rail deflection is insignificant when the wheelset is far away. The differences of the results obtained by the linear and non-linear track models are more obvious when the wheelset is close to mid-span (1.4–1.48 s). The maximum deflection obtained by the linear track model is larger than the one obtained by the non-linear model by approximately 8%.

The complete time histories of the rail acceleration at mid-span are compared in Fig. 8. The 0 s corresponds to the instant when the wheelset departs from the left boundary.

After the entry of the wheelset in the track model, the rail mid-span keeps still for about 0.03 s and then starts vibrating at relatively high frequency which approaches 180 Hz, as shown in (Fig. 8(a)). This high-frequency vibration is the transient response of the rail due to the entry of the wheelset and it took 0.03 s for the wave to propagate from the left model boundary to the rail mid-span. The result obtained by the non-linear track model has a higher maximum acceleration and decays much slower than the one of the linear track model, which is mainly due to the fact that the damping of the non-linear foundation is much lower than the one of the linear foundation in the concerned frequency range. When the force approaches and then crosses mid-span (Fig. 8(b)), besides the acceleration induced by the passage of the wheelset which gives the maximum acceleration of about  $5 \text{ m/s}^2$ , a vibration of 60 Hz appears in the result of the non-linear track model, which is associated with the dynamic coupling of the wheelset and a small portion of the rail around the position of the wheelset. When the force is near the right model boundary (Fig. 8(c)), the rail accelerations obtained by both models are insignificant compared to the maximum value of the complete time histories. However, it is obvious that the amplitude of the non-linear track model is much higher than the one of the linear track model due to the slower decay of the transient response.



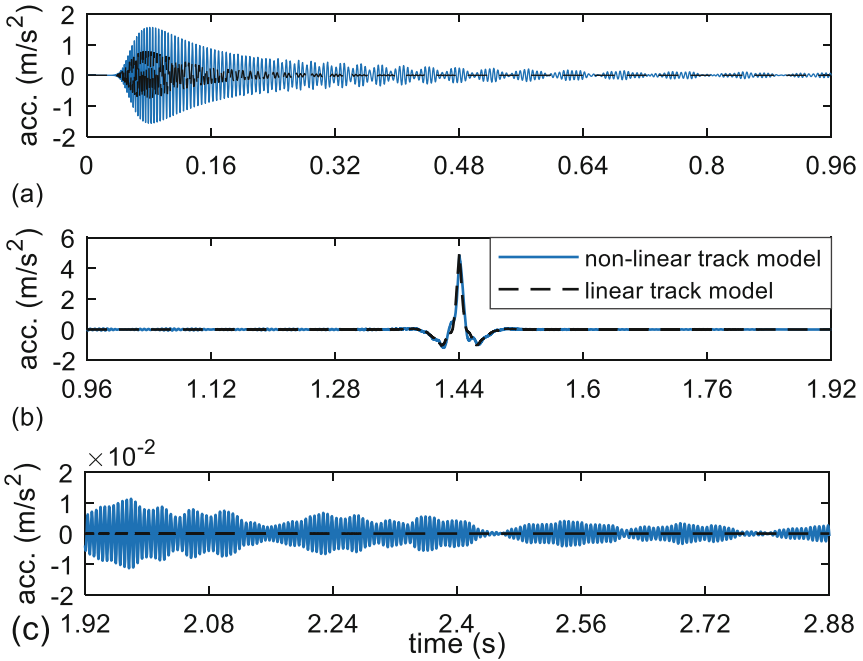


**Fig. 8.** Rail accelerations at mid-span of the track models corresponding to a passage of the wheelset of an ETR 500 train at 200 km/h, obtained with linear and non-linear track models: (a) time history of 0–0.96 s, (b) time history of 0.96–1.92 s and (c) time history of 1.92–2.88 s.

The spectrograms of the presented time histories are presented in Fig. 9. The length of the employed time window is 0.1 s and there is a 50% overlap between the adjacent windows.

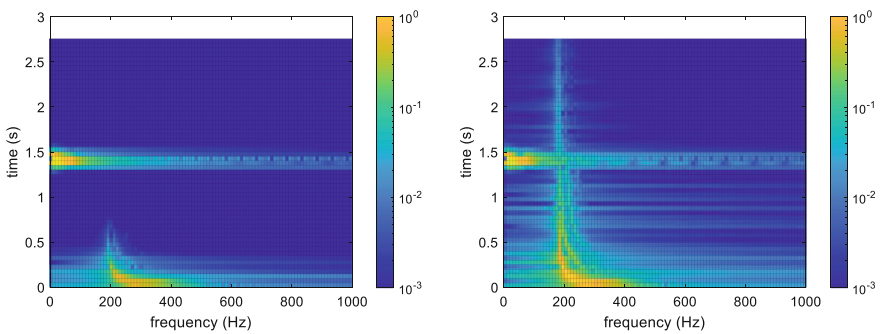


**Fig. 9.** Spectrograms of the rail accelerations at mid-span of the track models corresponding to a passage of the wheelset of an ETR 500 train at 200 km/h, obtained with linear (left) and non-linear track model (right). The length of time window is 0.1 s and the overlap between the adjacent windows is 50%.

The spectrograms show that the rail responses related to the passage of the wheelset over the mid-span are limited in a small time interval centred at the time instant of the passage. It is also better visualised that the transient response of the non-linear model lasts longer than the non-linear model.

The complete time histories of the wheelset displacement are compared in Fig. 10.

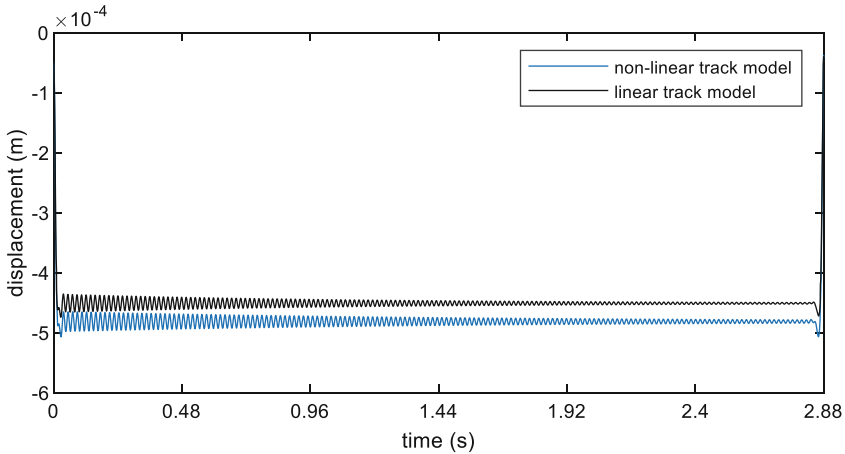


**Fig. 10.** Wheelset displacements corresponding to the passage of a wheelset of an ETR 500 train at 200 km/h on the linear and non-linear track models.

It can be observed that soon after the wheelset departs from the left boundary, the wheelset displacements tend to steady-state constant values independent of the type of the track model. The steady-state displacements are the maximum rail deflections induced by the passage of the wheelset shown in Fig. 7. The frequency of the transient responses present in both results (the small vibrations around the steady-state displacements) are of 60 Hz and are associated with the dynamic coupling of the wheelset and a small portion of the rail around the position of the wheelsets, corresponding to the 60 Hz vibration observed in the rail acceleration obtained with the non-linear track model in Fig. 8(b). The one of the non-linear track model decays slower than the one of the linear track model.

## 4 Conclusion

In this paper, the dynamic characteristics of an ERS are investigated through laboratory tests. The equivalent stiffness and damping show their strong dependence on the preload and frequency. A non-linear rheological model is identified with the experimental data and is proved an appropriate way for the modelling of the dynamic properties of the ERS. The rheological model is then integrated into a 2D track model and a wheelset-track dynamic interaction simulation was performed. The results, in terms of the track and the wheelset responses, show substantial differences from the ones obtained with the linear track model.

The differences between the results of the linear and non-linear track model imply that the non-linear dynamic properties of resilient materials should be carefully analysed and subsequently accounted for in the train-track dynamic interaction when an accurate prediction of the system response is desired. To this end, non-linear rheological models of the relevant track components can be developed from laboratory tests and then included in the train-track dynamic interaction models.

## References

1. Knothe, K.L., Grassie, S.L.: Modelling of railway track and vehicle/track interaction at high frequencies. *Veh. Syst. Dyn.* **22**, 209–262 (1993)
2. Sheng, X., Jones, C.J.C., Thompson, D.J.: A theoretical model for ground vibration from trains generated by vertical track irregularities. *J. Sound Vib.* **272**(3–5), 937–965 (2004)
3. Lombaert, G., Degrande, G., Kogut, J., François, S.: The experimental validation of a numerical model for the prediction of railway induced vibrations. *J. Sound Vib.* **297**(3–5), 512–535 (2006)
4. Zhai, W., Han, Z., Chen, Z., Ling, L., Zhu, S.: Train–track–bridge dynamic interaction: a state-of-the-art review. *Veh. Syst. Dyn.* **57**, 984–1027 (2019)
5. Sjöberg, M., Kari, L.: Non-linear behavior of a rubber isolator system using fractional derivatives. *Veh. Syst. Dyn.* **37**(3), 217–236 (2002)
6. Thompson, D.J., Verheij, J.W.: The dynamic behaviour of rail fasteners at high frequencies. *Appl. Acoust.* **52**, 1–17 (1997)
7. Bruni, S., Collina, A.: Modelling the viscoelastic behaviour of elastomeric components: an application to the simulation of train–track interaction. *Veh. Syst. Dyn.* **34**, 283–301 (2000)
8. Berg, M.: A model for rubber springs in the dynamic analysis of rail vehicles. *Proc. Insti. Mech. Eng. Part F: J. Rail Rapid Trans.* **211**, 95–108 (1997)
9. Fenander, Å.: A fractional derivative railpad model included in a railway track model. *J. Sound Vib.* **212**, 889–903 (1998)
10. Zhu, S., Cai, C., Spanos, P.: A nonlinear and fractional derivative viscoelastic model for rail pads in the dynamic analysis of coupled vehicle–slab track system. *J. Sound Vib.* **335**, 304–320 (2015)
11. Li, Q., Corradi, R., Di Gialleonardo, E., Bionda, S., Collina, A.: Testing and modelling of elastomeric element for an embedded rail system. *Materials (Basel)* **14**(22), 6968 (2021)
12. BS EN 13146-9:2009+A1: Railway applications—Track—Test methods for fastening systems. Part 9: determination of stiffness (2011)
13. De Man, A.P.: Dynatrack: a survey of dynamic railway track properties and their quality (2002)